湊川真理、室谷浩二、花川純子、大戸佑二、朝倉由美、安達昌功	生後7ヶ月に嘔吐と意識障害で発症したグルタル酸血症2型の一例	特殊ミルク情報	49	21-26	2013
土居美智子、近藤達郎、森藤香奈子、本村秀樹、増崎英明、松本正、森内浩幸	染色体異常児家族への告知に関しての家族・医師へのアンケート調査から見えてくるものー より良い告知の目指してー	日本周産期・新生児医学会雑誌	48(4)	897-904	2013
Fuke T, Mizuno S, Nagai T, Hasegawa T, Horikawa R, Miyoshi Y, Muroya K, Kondoh T, Numakura C, Sato S, Nakabayashi K, Tayama C, Hata K, Sano S, Matsubara K, Kagami M, Yamazawa K, Ogata T	Molecular and Clinical Studies in 138 Japanese Patientswith Silver-Russell Syndrome.	PLoS ONE	8(3)	e60105	2013
近藤達郎	先天性疾患の診断を伝える	小児科診療	76(7)	1061-1066	2013
森藤香奈子、佐々木規子、土居美智子、本村秀樹、森内浩幸、近藤達郎、松本正	染色体異常児家族が告知に望むものー構造構成的質的研究法によるアンケート調査自由記載の分析ー	日本周産期・新生児医学会雑誌	49(1)	227-232	2013
佐治勉、近藤達郎、与田仁志、森尾友宏	ダウン症候群とRSウィルス感染症の病態を考えるー各領域における現状と問題点ー	Fetal & Neonatal Medicine	5(2)	26-35	2013
Hirai M, Muramatsu Y, Mizuno S, Kurahashi N, Kurahashi H, Nakamura M.	Developmental changes in mental rotation ability and visual perspective-taking in children and adults with Williams syndrome.	Front Hum Neurosci	11	856	2013
Shimizu K, Wakui K, Kosho T, Okamoto N, Mizuno S, Itomi K, Hattori S, Nishio K, Samura O, Kobayashi Y, Kako Y, Arai T, Oh-Ishi T, Kawame H, Narumi Y, Ohashi H, Fukushima Y.	Microarray and FISH-based genotype-phenotype analysis of 22 Japanese patients with Wolf-Hirschhorn syndrome.	Am J Med Genet A.	2013	Dec 19.[Epub ahead of print]	[Epub ahead of print]
Nishi E, Takamizawa S, Iio K, Yamada Y, Yoshizawa K, Hatata T, Hiroma T, Mizuno S, Kawame H, Fukushima Y, Nakamura T, Kosho T.	Surgical intervention for esophageal atresia in patients with trisomy 18.	Am J Med Genet A.	2013	Dec 5.	[Epub ahead of print]

Hirai M, Muramatsu Y, Mizuno S, Kurahashi N, Kurahashi H, Nakamura M.	Developmental changes in mental rotation ability and visual perspective-taking in children and adults with Williams syndrome.	Front Hum Neurosci	11	856	2013
Shimizu K, Wakui K, Kosho T, Okamoto N, Mizuno S, Itomi K, Hattori S, Nishio K, Samura O, Kobayashi Y, Kako Y, Arai T, Oh-Ishi T, Kawame H, Narumi Y, Ohashi H, Fukushima Y.	Microarray and FISH-based genotype-phenotype analysis of 22 Japanese patients with Wolf-Hirschhorn syndrome.	Am J Med Genet A.	2013	Dec 19.[Epub ahead of print]	[Epub ahead of print]
Nishi E, Takamizawa S, Iio K, Yamada Y, Yoshizawa K, Hatata T, Hiroma T, Mizuno S, Kawame H, Fukushima Y, Nakamura T, Kosho T.	Surgical intervention for esophageal atresia in patients with trisomy 18.	Am J Med Genet A.	2013	Dec 5.	[Epub ahead of print]
Miyake N, Koshimizu E, Okamoto N, Mizuno S, Ogata T, Nagai T, Kosho T, Ohashi H, Kato M, Sasaki G, Mabe H, Watanabe Y, Yoshino M, Matsuishi T, Takanashi J, Shotelersuk V, Tekin M, Ochi N, Kubota M, Ito N, Ihara K, Hara T, Tonoki H, Ohta T, Saito K, Matsuo M, Urano M, Enokizono T, Sato A, Tanaka H, Ogawa A, Fujita T, Hiraki Y, Kitanaka S, Matsubara Y, Makita T, Taguri M, Nakashima M, Tsurusaki Y, Saitsu H, Yoshiura K, Matsumoto N, Niikawa N.	MLL2 and KDM6A mutations in patients with Kabuki syndrome.	Am J Med Genet A.	161 (9)	2234-43	2013
Suzumori N, Kaname T, Muramatsu Y, Yanagi K, Kumagai K, Mizuno S, Naritomi K, Saitoh S, Sugiura-Ogasawara M.	Prenatal diagnosis of X-linked recessive Lenz microphthalmia syndrome.	J Obstet Gynaecol Res.	39(11)	1545-7	2013

Ⅴ．研究成果の刊行物・別刷

CLINICAL REPORT

AMERICAN JOURNAL OF medical genetics PART A

Pure Duplication of 19p13.3

Aki Ishikawa,[1] Keisuke Enomoto,[1] Makiko Tominaga,[1] Toshiyuki Saito,[2] Jun-ichi Nagai,[2] Noritaka Furuya,[1] Kentaro Ueno,[3] Hideaki Ueda,[3] Mitsuo Masuno,[4] and Kenji Kurosawa[1,5]*

[1]Division of Medical Genetics, Kanagawa Children's Medical Center, Yokohama, Japan

[2]Department of Clinical Laboratory, Kanagawa Children's Medical Center, Yokohama, Japan

[3]Department of Pediatric Cardiology, Kanagawa Children's Medical Center, Yokohama, Japan

[4]Genetic Counseling Program, Graduate School of Health and Welfare, Kawasaki University of Medical Welfare, Kurashiki, Japan

[5]Institute for Clinical Research, Kanagawa Children's Medical Center, Yokohama, Japan

Manuscript Received: 10 June 2012; Manuscript Accepted: 15 April 2013

Chromosomal abnormalities involving 19p13.3 have rarely been described in the published literature. Here, we report on a girl with a pure terminal duplication of 6.1 Mb on 19p13.3, caused by an unbalanced translocation der(19)t(10;19)(qter;p13.3)dn. Her phenotype included severe psychomotor developmental delay, skeletal malformations, and a distinctive facial appearance, similar to that of a patient previously reported by Lybaek et al. [Lybaek et al. (2009); Eur J Hum Genet 17:904–910]. These results suggest that a duplication of >3 Mb at the terminus of 19p13.3 might represent a distinct chromosomal syndrome.

Key words: 19p13.3 duplication; array CGH; developmental delay; subtelomere

How to Cite this Article:
Ishikawa A, Enomoto K, Tominaga M, Saito T, Nagai J, Furuya N, Ueno K, Ueda H, Masuno M, Kurosawa K. 2013. Pure duplication of 19p13.3.
Am J Med Genet Part A 161A:2300–2304.

INTRODUCTION

Chromosome 19 is more gene-dense than any other human chromosome. Non-mosaic 19p trisomy is a rare chromosomal aberration, of which only 9 occurrences have been reported to date [Byrne et al., 1980; Salbert et al., 1992; Stratton et al., 1995; Andries et al., 2002; Puvabanditsin et al., 2009; Lybaek et al., 2009; Descartes et al., 2011; Siggberg et al., 2011; Lehman et al., 2012]. More specifically, pure and non-mosaic trisomy of 19p has been reported in only five of these patients [Stratton et al., 1995; Andries et al., 2002; Lybaek et al., 2009; Siggberg et al., 2011; Lehman et al., 2012].

Here, we report on a 3-year-old girl with pure terminal duplication of 19p13.3, confirmed using FISH and array CGH. She had multiple malformations, including a complex congenital heart defect, a distinctive facial appearance, and severe developmental delay. Taken together, our findings, along with a review of the literature, allow clarification of a more precise and comprehensive phenotype–genotype correlation for pure 19p duplication.

CLINICAL REPORT

The proposita is the first child of healthy unrelated parents with unremarkable family history. At the time of delivery, the mother was 36 years old, and the father was 27 years old. The pregnancy was complicated by intrauterine growth retardation first noted at 27 weeks. The infant was delivered at 35 weeks of gestation by cesarean due to fetal distress. Her birth weight was 1,216 g; length, 36.5 cm; and occipitofrontal circumference (OFC), 28.0 cm. Her Apgar scores were 4 at 1 min, and 9 at 5 min. Because of her very low birth weight and respiratory failure, she was admitted to a neonatal intensive care unit. Initial physical examination showed a distinctive facial appearance with micrognathia, low-set ears, and a prominent occiput. An echocardiogram revealed a complete atrioventricular septal defect of Rastelli A type, severe pulmonary hypertension, and mitral valve dysplasia.

At the age of 8 months, catheter examination demonstrated that an operative procedure was not indicated for her heart defects; conservative treatment with beraprost sodium and bosentan hydrate, in addition to oxygen supplementation, was adopted for heart failure and severe pulmonary hypertension. From the age of 1 year and 8 months, sildenafil citrate was also added to her treatment. At this age, she had marked cardiac failure and had experienced several episodes of recurrent respiratory infection.

Grant sponsor: Research on Measures for Intractable Diseases Project, The Ministry of Health, Labour and Welfare, Japan.
*Correspondence to:
Kenji Kurosawa, M.D., Ph.D., Division of Medical Genetics, Kanagawa Children's Medical Center, 2-138-4 Mutsukawa, Minami-ku, Yokohama 232-8555, Japan. E-mail: kkurosawa@kcmc.jp
Article first published online in Wiley Online Library (wileyonlinelibrary.com): 29 July 2013
DOI 10.1002/ajmg.a.36041

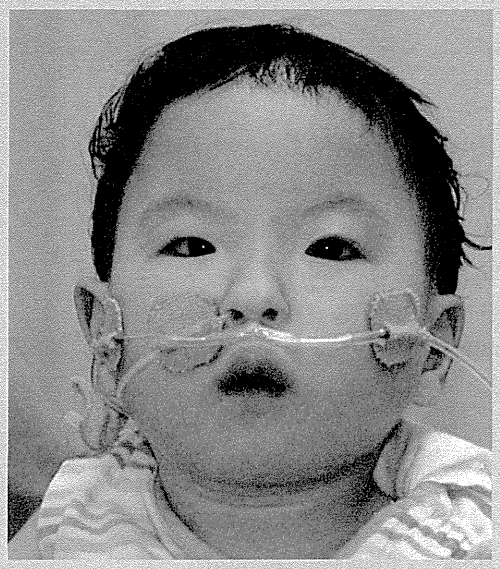

FIG. 1. Patient at the age of 3 years, showing strabismus, short palpebral fissures, hypoplastic nasal alae, low-set ears, and microstomia.

On examination at the age of 3 years, her weight was 7,680 g (−3.4 SD); height, 75 cm (−5.0 SD); and OFC, 42 cm (−4.0 SD) (Fig. 1). Her facial appearance showed strabismus, short and downslanting palpebral fissures, microcephaly, hypoplastic nasal alae, sparse scalp hair, and eyebrows, low-set ears, a short philtrum, protruding upper lip, and microstomia with micrognathia. Orthopedic examination showed kyphoscoliosis and dislocation of bilateral hip joints. Her development was severely delayed. She could roll over and required gavage feeding. Her heart failure progressed, and died at age 4 years. Postmortem examination revealed an ectopic left kidney in front of the vertebrae.

MATERIALS AND METHODS

Written informed consent was obtained from the parents of the patient, and the study was performed in accordance with the Kanagawa Children's Medical Center Review Board and Ethics Committee.

An initial FISH analysis for patients with developmental delay/intellectual disability (DD/ID) and/or multiple congenital anomalies (MCA) was carried out using subtelomeric probes (Vysis, Downers Grove, IL) according to the standard protocol. Further FISH analysis for determining the breakpoint on 19p13.3 was carried out using bacterial artificial chromosome (BAC) clones that had been selected from the May 2004 (NCBI35/hg17). Human assembly of the UCSC Genome Browser (http://genome.ucsc.edu/). A centromeric probe specific for chromosome 10 was used to confirm chromosome 10. The BAC clones were labeled by nick translation according to the manufacturer's instructions (Vysis, Downers Grove, IL). Hybridization, post-hybridization washing, and counterstaining were performed according to standard procedures. Slides were analyzed using a completely motorized epifluorescence microscope (Leica DMRXA2; Leica Microsystems Imaging Solutions, Cambridge, UK) equipped with a CCD camera. Both the camera and microscope were controlled with Leica CW4000 M-FISH software [Yamamoto et al., 2009].

Array comparative genomic hybridization (array-CGH) was performed using the Agilent SurePrint G3 Human CGH Microarray Kit 8 × 60K (Agilent Technologies, Inc., Santa Clara, CA). The total genomic DNA of the patient was prepared using standard techniques. The results were analyzed using Agilent Genomic Workbench software. Only experiments having a derivative log ratio (DLR) spread value <0.30 were considered.

RESULTS

The complete subtelomere probe set analysis detected an additional signal for 19pter on the terminal of the long arm in group C chromosomes in the patient. Based on the results of the G-banding patterns and FISH with a centromeric probe, the derivative chromosome was determined to be chromosome 10 (Fig. 2a,b). However, the 10qter probe signal was retained in the derivative chromosome (data not shown). To characterize the size of the deletion, we further applied FISH analysis using the BAC clones that mapped to the region. This revealed that the breakpoint was 6.1 Mb from 19pter (Table I). Subsequent array-CGH analysis revealed a 19p13.3 duplication of approximately 6.1 Mb (chr19: 327,273–6,106,229), which was consistent with the FISH results (Fig. 2c). No other genomic imbalances were identified on the array analysis. FISH analysis with relevant BAC clones indicated that the duplication was absent in both parents, and therefore had occurred de novo.

DISCUSSION

Reports of abnormalities of the short arm chromosome 19 are rare; to date, only nine patients with non-mosaic duplication of 19p have been reported. Of these, four involved translocation of other chromosomes [Byrne et al., 1980; Salbert et al., 1992; Puvabanditsin et al., 2009; Descartes et al., 2011], and only five patients had a pure partial duplication of 19p [Stratton et al., 1995; Andries et al., 2002; Lybaek et al., 2009; Siggberg et al., 2011; Lehman et al., 2012] (Fig. 3., Table II). This report is, to our knowledge, only the second report of a pure terminal duplication of 19p13.3.

Array-CGH and FISH analysis refined the breakpoint at 6.1 Mb from 19pter. Three patients harboring a duplication of more than 1 Mb at 19p13.3 have been recorded on the DECIPHER database (https://decipher.sanger.ac.uk/), but no individual with a duplication of more than 3 Mb is recorded therein. Fourteen patients having a duplication of a fragment of 19p13.3 have been reported in the database of International Standards for Cytogenetic Arrays Consortium (ISCA). The phenotypical manifestations of these patients consist of multiple congenital abnormalities and seizures. However, the detailed phenotypic features of the patients were not available. Although the phenotype deriving from duplication of a limited region of 19pter is not always recognizable [Andries

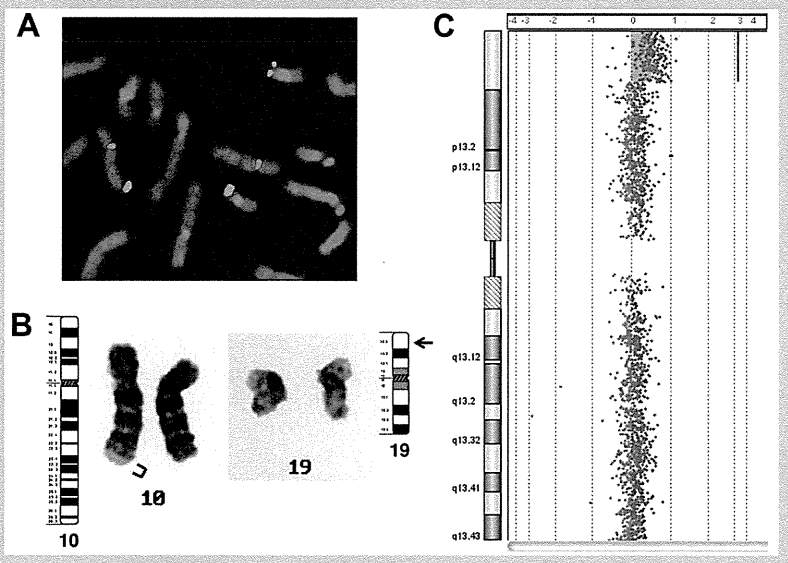

FIG. 2. FISH and array-CGH characterization of 19p13.3 terminal duplication. A: FISH image showing an additional signal at 10qter. BAC probe RP11-43H17 from the duplicated region of 19p13.3 is labeled in green, and chromosome 10 centromeric probe (Vysis, CEP10) is labeled in red, as a control. B: G-banded metaphase chromosomes, showing der(10)t(10;19)(qter;p13.3). C: Array-CGH showing duplication of 19p13.3. The region extends to position 6,106,229 according to UCSC human genome assembly build 19.

et al., 2002], the present case presented with severe psychomotor disability, no verbal language use, a distinctive facial appearance, and skeletal features including small hands and feet and bilateral hip dysplasia. These phenotypic features, especially the characteristic facial appearance, were also shared by the patient described by Lybaek et al. [2009]. The patient had a small mouth, short philtrum, full cheek, short palpebral fissures, and the extreme precocious puberty before the age of 5 months. They demonstrated that only about 25% of the duplicated 215 genes presented the overall expression pattern by more than 1.3-fold, and suggested no genes might explain the precocious puberty characterized in their patient. However, our present patient had no symptom of early puberty observed by the age of 4 years.

TABLE I. FISH Results Around the Breakpoint of the Translocation

BAC clones	Position from 19pter[a]	FISH results
RP11-1051P16	3,421,215–3,617,048	×3
RP11-43H17	4,318,718–4,491,568	×3
RP11-348B12	4,960,407–5,144,570	×3
RP11-294F21	5,854,144–6,041,711	×3
RP11-576B17	6,172,183–6,249,454	×3
RP11-114A7	6,199,888–6,359,433	×2
RP11-30F17	6,351,112–6,519,252	×2
RP11-459P1	6,396,557–6,544,479	×2
RP11-526C20	6,450,800–6,626,432	×2
RP11-222E10	6,560,463–6,759,394	×2
RP11-441C15	7,891,868–8,086,997	×2

[a]Positions of the BAC clones were based on the May 2004 (NCBI35/hg17) Human Assembly of the UCSC Genome Browser (http://genome.ucsc.edu/).

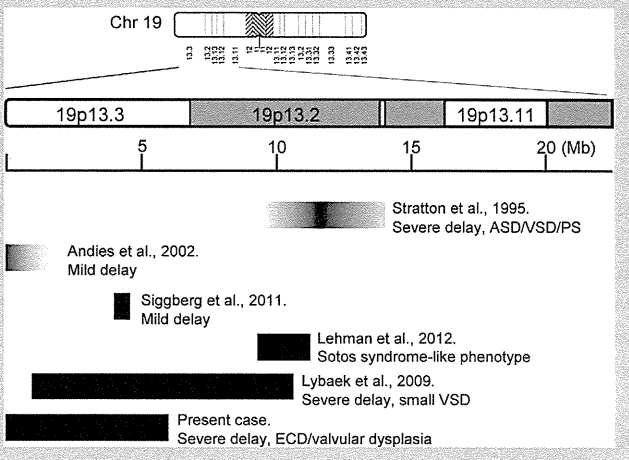

FIG. 3. Schematic representation of the microduplication on 19p13.3. The dark horizontal bars indicate the range of the duplication in reported patients. The duplicated regions in the patients reported by Stratton et al. [1995] and Andries et al. [2002] were ascertained from the respective reports.

TABLE II. Summary of Clinical Features in Five Individuals With Pure Microduplication at 19p13

	Stratton et al. [1995]	Andries et al. [2002]	Siggberg et al. [2011]	Lehman et al. [2012]	Lybaek et al. [2009]	Present patient
Age, sex	9 months, F	20 months, F	9 yrs, M	1–74 yrs, M/F	2 ½ yrs, F	3yrs, F
Karyotype	dup(19) (p13.2p13.13)	der(14)t (14;19) (q32.3;p13.3)	dup(19) (p13.3p13.3)	dup(19) (p13.2p13.2)	ins(19) (q13.3p13.2-p13.3)	der(10)t (10;19) (qter;p13.3)
Duplication	p13.2–p13.13	pter-p13.3	p13.3, 0.81 Mb	p13.2. 1.9 Mb	p13.3–p13.2, 8.9 Mb	p13.3, 6.10 Mb
(from pter)	?	?	(3.927–4.471 Mb)	(9.109–11.068 Mb)	(1.4–10.3 Mb)	(–6.106 Mb)
Pattern	Interstitial	Terminal	Interstitial	Interstitial	Interstitial	Terminal
Gestational age	Term	41 wks	Term	Term	35 wks	35 wks
Birth weight	2,730 g		2,730 g	4,550 g	1,790 g	1,216 g
Growth retardation	+	–	+	–	+	+ Severe
Development	Delay	Mild delay	Mild delay	Mild delay	Severe delay	Severe delay
Cardiovascular	PS, ASD, VSD	—	—	—	small VSD	ECD, PH, valvular dysplasia
Others	Strabismus, nail hypoplasia	Sparse hair, low-set ears, short nose	Amblyopia	Sotos syndrome-like	Severe eating problem, congenital hip dysplasia	Strabismus, renal aplasia (L), vertebral defects, nail hypoplasia, dislocation of hip joint

Thus, a duplication of >3 Mb of the terminal region of 19p13.3 might contribute to a more severe phenotype than do smaller duplications, and this phenotype might be characteristic of this chromosomal aberration.

Accurate assessment of the duplication size enabled us to evaluate the genes located within the duplicated region, which presumably contribute to the phenotypes. The duplicated region contains approximately 150 RefSeq genes and 130 OMIM genes, 18 of which have known disease associations. However, this case demonstrates that evaluation of the gene content of a chromosomal region is not sufficient to assess the pathogenicity of a gene duplication. Additional reports of individuals with this chromosomal aberration are required to demonstrate genotype–phenotype correlation in 19p duplication.

ACKNOWLEDGMENTS

We thank the patient and her family for making this study possible. The authors thank Dr. Yoshikazu Kuroki (Kanagawa Children's Medical Center, Yokohama, Japan) for his valuable comments. This research was supported in part by a "Research on Measures for Intractable Diseases" project: Matching funds subsidy from the Ministry of Health, Labor and Welfare, Japan.

REFERENCES

Andries SA, Sartenaer D, Rack K, Rombout S, Tuerlinckx D, Gillerot Y, van Maldergem L. 2002. Pure terminal duplication of the short arm of chromosome 19 in a boy with mild microcephaly. J Med Genet 39:e60.

Byrne JLB, Korn GA, Dev VG, Bunch GM, Brooks K, Friedman JM, Harrod MJE. 1980. Partial trisomy 19p. Am J Hum Genet 32:64A.

Descartes M, Mikhail FM, Franklin JC, McGrath TM, Bebin M. 2011. Monosomy 1p36.3 and trisomy 19p13.3 in a child with periventricular nodular heterotopias. Pediatr Neurol 45:274–278.

Lehman AM, du Souich C, Chai D, Eydoux P, Huang JL, Fok AK, Avila L, Swingland J, Delaney AD, McGillivray B, Goldowitz D, Argiropoulos B, Kobor MS, Boerkoel CF. 2012. 19p13.2 microduplication causes a Sotos syndrome-like phenotype and alters gene expression. Clin Genet 81: 56–63.

Lybaek H, Orstavik KH, Prescott T, Hovland R, Breilid H, Stansberg C, Steen VM, Houge G. 2009. An 8.9 Mb 19p13 duplication associated with precocious puberty and a sporadic 3.9Mn 2q23.2q24.1 deletion containing *NR4A2* in mentally retarded members of a family with an intrachromosomal 19p-into-19q between-arm insertion. Eur J Hum Genet 17:904–910.

Puvabanditsin S, Garrow E, Brandsma E, Savla J, Kunjumon B, Gadi I. 2009. Partial trisomy 19p13.3 and partial monosomy 1p36.3: Clinical report and a literature review. Am J Med Genet Part A 149A:1782–1785.

Salbert BA, Solomon M, Spence JE, Jackson-Cook C, Brown J, Bodurtha J. 1992. Partial trisomy 19p: Case report and natural history. Clin Genet 41:143–146.

Siggberg L, Olsen P, Kanto-Salonen K, Knuutila S. 2011. 19p13.3 aberrations are associated with dysmorphic features and deviant psychomotor development. Cytogenet Genome Res 132:8–15.

Stratton RF, DuPont BR, Olsen AS, Fertitta A, Hoyer M, Moore CM. 1995. Interstitial duplication 19p. Am J Med Genet 57:562–564.

Yamamoto K, Yoshihashi H, Furuya N, Adachi M, Ito S, Tanaka Y, Masuno M, Chiyo H, Kurosawa K. 2009. Further delineation of 9q22 deletion syndrome associated with basal cell nevus (Gorlin) syndrome: Report of two cases and review of the literature. Congenit Anom (Kyoto) 49:8–14.

Adachi et al. Journal of Medical Case Reports 2013, 7:283
http://www.jmedicalcasereports.com/content/7/1/283

JOURNAL OF MEDICAL CASE REPORTS

CASE REPORT Open Access

Classic Bartter syndrome complicated with profound growth hormone deficiency: a case report

Masanori Adachi[1*], Toshihiro Tajima[2], Koji Muroya[1] and Yumi Asakura[1]

Abstract

Introduction: Classic Bartter syndrome is a salt-wasting tubulopathy caused by mutations in the *CLCNKB* (chloride channel Kb) gene. Although growth hormone deficiency has been suggested as a cause for persistent growth failure in patients with classic Bartter syndrome, in our opinion the diagnoses of growth hormone deficiency has been unconvincing in some reports. Moreover, Gitelman syndrome seems to have been confused with Bartter syndrome in some cases in the literature. In the present work, we describe a new case with *CLCNKB* gene mutations and review the reported cases of classic Bartter syndrome associated with growth hormone deficiency.

Case presentation: Our patient was a Japanese boy diagnosed as having classic Bartter syndrome at eight months of age. The diagnosis of Bartter syndrome was confirmed by *CLCNKB* gene analysis, which revealed compound heterozygous mutations with deletion of exons 1 to 3 (derived from his mother) and ΔL130 (derived from his father). His medical therapy consisted of potassium (K), sodium chloride, spironolactone, and anti-inflammatory agents; this regime was started at eight months of age. Our patient was very short (131.1cm, -4.9 standard deviation) at 14.3 years and showed profoundly impaired growth hormone responses to pharmacological stimulants: 0.15μg/L to insulin-induced hypoglycemia and 0.39μg/L to arginine. His growth response to growth hormone therapy was excellent.

Conclusions: The present case strengthens the association between classic Bartter syndrome and growth hormone deficiency. We propose that growth hormone status should be considered while treating children with classic Bartter syndrome.

Keywords: Bartter syndrome, Salt-losing tubulopathy, Hypokalemia, Gitelman syndrome, Growth failure

Introduction

Classic Bartter syndrome (BS), also referred to as type III Bartter syndrome, is a rare genetic disorder characterized by salt wasting from the renal tubules, mainly the thick ascending loop of Henle [1]. It is caused by mutations in the *CLCNKB* gene that encodes the type b kidney chloride channel (ClC-Kb). Patients with classic BS fail to thrive from infancy and exhibit hypokalemia, metabolic alkalosis, hyperactive renin-aldosterone system, and overproduction of prostaglandins. Although potassium supplements, anti-aldosterone agents, and/or indomethacin are the mainstay of therapy, management of growth failure and hypokalemia is still challenging [1,2].

The association of growth hormone deficiency (GHD) with classic BS has been anecdotally reported, and GHD may be one of the causes of persistent growth failure frequently observed in patients with classic BS [2-8]. However, the degrees of GHD in the reported cases have been diverse, and hence, GHD has not yet been regarded as a definite complication of BS. In addition, most of the reported cases of BS accompanying GHD were not investigated on a molecular basis [3,7,8]. Moreover, Gitelman syndrome (GS) seems to have been confused with BS in older reports in the literature [4-6]. Here, we report a case of classic BS with documented *CLCNKB* gene mutations in a boy who was found to have profound

* Correspondence: madachi@mars.sannet.ne.jp
[1]Department of Endocrinology and Metabolism, Kanagawa Children's Medical Center, Mutsukawa 2-138-4 Minami-ku, Yokohama 232-8555, Japan
Full list of author information is available at the end of the article

GHD. We also present a literature review on the association between classic BS and GHD.

Case presentation

Our patient was a Japanese boy born at 41 weeks of gestation via spontaneous cephalic delivery, with a birth weight of 3,680g. His family history was remarkable in that his elder sister, who was five years older than him, had been diagnosed as having classic BS when she was five months old: her final height was 147.0cm (−2.1 standard deviation [SD]) and at a recent assessment her insulin-like growth factor 1 (IGF-1) level was 286ng/mL (normal range for her age, 168 to 459ng/mL).

At eight months of age, our patient was diagnosed as having classic BS based on the following findings: failure to thrive, metabolic alkalosis (pH 7.423; HCO_3^-, 33.6mmol/L; base excess, +8.2), hypokalemia (2.9mEq/L), and hyperactive renin-aldosterone system (plasma renin activity (PRA), 270ng/mL/h; normal value for his age, 2.58 ± 1.41ng/mL/h); aldosterone level, 850pg/mL (2,358pmol/L; normal value for his age, 173.7 ± 96.3pg/mL). The diagnosis of BS was confirmed by *CLCNKB* gene analysis, which revealed compound heterozygous mutations with deletion of exons 1 to 3 (derived from his mother) and ΔL130 (derived from his father), the latter of which has been reported previously by the authors TT and MA. Medical therapy consisting of potassium (K), sodium chloride, spironolactone, and anti-inflammatory agents was initiated at eight months of age and is still ongoing. However, as depicted in Figure 1, his serum K level remained considerably low because he was unable to consume large amounts of drugs, especially potassium preparations. Our patient also displayed mild intellectual impairment: he could only speak meaningful words by the age of three, and required specialized primary education.

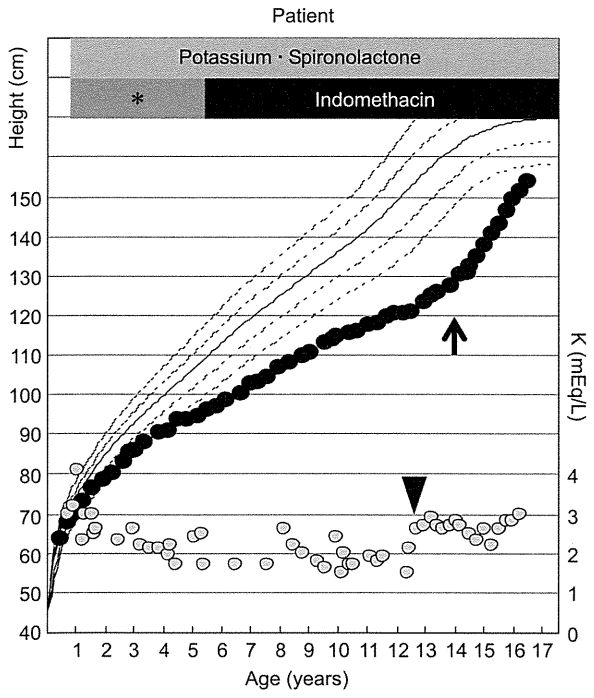

Figure 1 Growth charts of our patient superimposed with variations in his serum potassium levels. Black circles indicate heights; gray circles indicate potassium levels. The arrowhead indicates the age at which our patient could ingest potassium tablets, allowing higher potassium levels than before. Arrow indicates the initiation of growth hormone therapy. *Non-indomethacin anti-inflammatory agents such as tolmetin sodium and mefenamic acid.

Table 1 Results of pharmacological growth hormone stimulation tests in our patient at 14 years of age

	0 minutes	30 minutes	60 minutes	90 minutes	120 minutes
Insulin-induced hypoglycemia:					
Blood glucose (mg/dL)	94	54	93	99	92
Growth hormone (μg/L)	0.11	0.07	0.15	0.13	0.08
Arginine:					
Growth hormone (μg/L)	0.11	0.26	0.39	0.28	0.17

When he was 11 years old, an investigation for macrohematuria led to the detection of renal stones with nephrocalcinosis. This complication resolved following the amelioration of hypokalemia, which was achieved by our patient's increased efforts to ingest potassium tablets.

At 14.3 years of age, his severe short stature (131.1cm, -4.9SD) prompted us to evaluate his growth

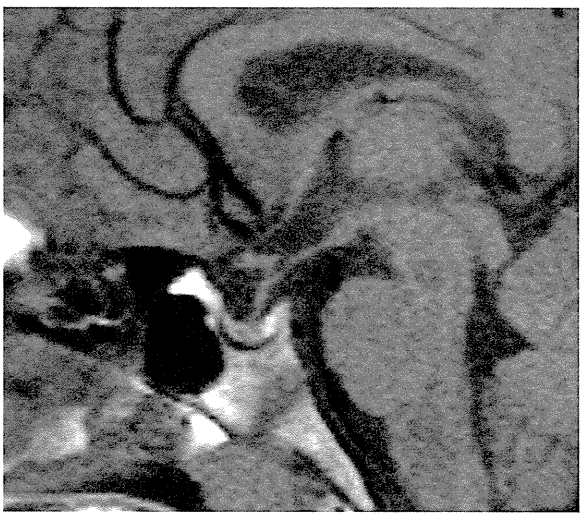

Figure 2 Magnetic resonance imaging scan of the pituitary gland of our patient.

Table 2 Classical Bartter syndrome with growth hormone deficiency: cases from the literature

Reference	Age, years	Sex	Mutation	GH peak (μg/L) to stimulants	IGF-1 (ng/mL)
[9]	5	M	IVS2-1G > C/W610X	9.3 (GLC), 8.0 (CLN), 8.2 (L-DOPA), 38.0 (ARG)	Not determined
[10]	8	F	Not determined	2.9 (INS), 2.0 (CLN), 6.9 (GRF)	122.1
[7]	10	M	Not determined	3.20 (INS), 3.20 (L-DOPA)	25
[8]	10	F	Not determined	0.70 (L-DOPA), 1.96 (CLN)	41.5
	11	M	Not determined	4.70 (L-DOPA), 1.79 (CLN)	39.7
	11	M	Not determined	0.50 (L-DOPA), 4.49 (CLN)	38.3
[2]	11	M	ΔExon1-6/ΔExon1-6	7.6 (ARG)	Low
	14	M	ΔExon1-19/ΔExon1-19	2.4 (ARG), 8.4 (GRF)	Low
[3]	22	F	Not determined	Absence (INS), 8.0 (ARG)	Not determined
Present case	14	M	ΔL130/ΔExon1-3	0.15 (INS), 0.39 (ARG)	80

ARG arginine, *CLN* clonidine, *L-DOPA* L-3,4-dihydroxyphenylalanine, *GH* growth hormone, *GLC* glucagon, *GRF*, growth hormone releasing factor, *IGF-1* insulin-like growth factor 1, *INS* insulin.

hormone (GH) status, and he was found to have profound GHD. His serum levels of IGF-1 and IGF binding protein 3 were 80ng/mL (normal range for his age, 178 to 686ng/mL) and 1.92μg/mL (normal range for his age, 2.69 to 4.16μg/mL), respectively. Pharmacologically stimulated GH levels were 0.15 and 0.39μg/L after insulin-induced hypoglycemia and arginine administration, respectively (Table 1). His bone age was 11.4 years (Tanner-Whitehouse 2-radius, ulna and short bones (TW2-RUS) method for Japanese individuals). Magnetic resonance imaging study results revealed no abnormalities in the hypothalamic-pituitary region (Figure 2).

GH therapy was initiated at 14.5 years of age at a dose of 21 to 27μg/kg/day, which restored his growth remarkably (Figure 1). Although his pubertal stage progressed from Tanner stage 1 to stage 2 over the next two years, his bone maturation (Δbone age/Δchronological age) was 1.02. No significant change was observed in his serum potassium level during GH therapy.

Discussion

To the best of our knowledge, the association of BS with GHD was first reported in 1977 [3]. Thereafter, a number of similar reports have been published [2-8]. However, we believe that some of the older cases reported in the literature do not comply with the current definition and concept of BS and thus should be recognized as GS [4-6]. GS is another salt-losing tubulopathy caused by mutations in the *SLC12A3* gene that encodes the thiazide-sensitive sodium-chloride cotransporter (NCCT) [1]. Because classic BS and GS shared the laboratory finding of hypokalemic alkalosis, these conditions were not strictly discriminated until the era of molecular diagnosis.

Table 3 Gitelman syndrome (including definite or probable cases) and GHD: cases from the literature

Reference	Age, years	Sex	Mutation	GH peak (μg/L) to stimulants	IGF-1
[12]	3	M	2614fr/unknown (*SLC12A3*)	<8 (INS), <8 (ARG), <8 (CLN)	Not determined
	9	F	G186D/unknown (*SLC12A3*)	6 (CLN)	89ng/mL
[5]	3	M	Not determined	3.3 (L-DOPA), 7.3 (CLN)	0.26U/mL
	9	F	Not determined	9.2 (L-DOPA), 4.8 (CLN)	0.67U/mL
	19	F	Not determined	6.0 (CLN)	Not determined
[6]	7	M	Not determined	9.8 (INS + ARG)	Not determined
[11]	9	M	Not determined	2.1 (INS), 3.2 (CLN), 1.8 (L-DOPA)	55ng/mL
[13]	10	F	Not determined	7.5 (L-DOPA), 6.9 (CLN)	Normal
[14]	11	M	Not determined	10.8 (GRF), 7.0 (CLN)	0.43U/mL
[15]	11	M	Not determined	5 (INS), 1 (CLN), 13 (GRF)	292ng/mL
[4]	11	M	Not determined	11 (CLN), 3.1 (GLC)	0.74U/mL
[16]	13	M	Not determined	5.4 (INS), 5.4 (ARG), 12 (GLC-PPL)	0.19U/mL

Cases were categorized as Gitelman syndrome according to the authors' own judgment, even if they were described as Bartter syndrome in the original reports. *ARG* arginine, *CLN* clonidine, *L-DOPA* L-3,4-dihydroxyphenylalanine, *GH* growth hormone, *GLC* glucagon, *GRF* growth hormone releasing factor, *IGF-1* insulin-like growth factor 1, *INS* insulin, *PPL* propranolol.

Molecular diagnosis is a prerequisite for the detailed study of classic BS.

Tables 2 and 3 summarize cases of GHD reported to date classified as BS [2,3,7-10] and GS [4-6,11-16], respectively. Our patient's case is remarkable in that the diagnosis of classic BS was established molecularly. In addition, our patient's GH responses to pharmacological stimulants were most profoundly impaired among the hitherto reported cases. Although one may argue that hypokalemia may blunt the GH response and lead to false negative results, the excellent response to GH therapy made us suspicious for the presence of GHD. By adding our patient to the existing list of cases of GHD concomitant with BS, we believe that GHD should be regarded as a complication in classic BS.

Flyvbjerg *et al.* suggested that hypokalemia is a causative factor of GHD [17]. These authors stated that mice fed a low potassium diet showed growth retardation with low IGF-1 levels and attenuated GH response to GH-releasing factor (GRF). From this observation, hypokalemia seems to be one of the possible factors responsible for GHD in classic BS. This hypothesis is strengthened by the findings that GHD has also been reported in other diseases predisposing to hypokalemia, such as GS (Table 3) and the Bartter-like Dent disease [18]. In addition, this hypothesis can help to differentiate GHD (our patient in the present report) from non-GHD (his sister). Because large amounts of potassium could be administered via the gastric tube or tablets, a higher serum potassium level could be maintained in the sister, which may have prevented the development of GHD. Furthermore, the lack of association between GHD and antenatal BS, which is caused by mutations in either the *SLC12A1* (type I BS) or *KCNJ1* (type II BS) gene, can be explained by the observation that the correction of hypokalemia is generally easier in antenatal BS than in classic BS.

However, factors other than hypokalemia may be necessary for developing GHD. Patients with familial aldosteronism, rare genetic forms of primary aldosteronism, present with hypokalemia and some of them are refractory to medical therapy, yielding to long standing hypokalemia [19]. Regardless, GHD has not been reported to date in patients with familial aldosteronism. Thus, an aim of our future studies would be to determine the precise mechanism by which GHD develops in patients with classic BS.

Conclusions

In summary, we report our experience of profound GHD in a boy with mutations in the *CLCNKB* gene, and propose that GH status should be monitored while treating salt-losing tubulopathies including classic BS and GS.

Consent

Written informed consent was obtained from the patient's next-of-kin for publication of this case report and any accompanying images. A copy of the written consent is available for review by the Editor-in-Chief of this journal.

This study was approved by the Institutional Review Board of Kanagawa Children's Medical Center and followed the World Medical Association Declaration of Helsinki regarding ethical conduct of research involving human subjects.

Abbreviations

BS: Bartter syndrome; GH: Growth hormone; GHD: GH deficiency; GRF: GH-releasing factor; GS: Gitelman syndrome; IGF-1: Insulin-like growth factor 1.

Competing interests

The authors declare that they have no competing interests.

Authors' contributions

MA treated our patient from the beginning, performed the *CLCNKB* gene analysis and evaluated the GH status of our patient. MA also wrote the manuscript. TT and KM planned and performed the *CLCNKB* gene analysis. YA and KM critically reviewed and revised the manuscript. All authors read and approved the final manuscript.

Acknowledgements

We thank Ms Reiko Iwano, Department of Endocrinology and Metabolism, Kanagawa Children's Medical Center, Japan, for her excellent technical assistance.

Author details

[1]Department of Endocrinology and Metabolism, Kanagawa Children's Medical Center, Mutsukawa 2-138-4 Minami-ku, Yokohama 232-8555, Japan. [2]Department of Pediatrics, Hokkaido University School of Medicine, Sapporo 060-8635, Japan.

Received: 12 August 2013 Accepted: 28 October 2013
Published: 30 December 2013

References

1. Seyberth HW, Schlingmann KP: **Bartter- and Gitelman-like syndromes: salt-losing tubulopathies with loop or DCT defects.** *Pediatr Nephrol* 2011, **26**:1789–1802.
2. Bettinelli A, Borsa N, Bellantuono R, Syrèn ML, Calabrese R, Edefonti A, Komninos J, Santostefano M, Beccaria L, Pela I, Bianchetti MG, Tedeschi S: **Patients with biallelic mutations in the chloride channel gene CLCNKB: long-term management and outcome.** *Am J Kidney Dis* 2007, **49**:91–98.
3. Lefebvre J, Racadot A, Dequiedt P, Linquette M: **Électrolytes échangeables, glycorégulateur et hormone de croissance au cours d'un syndrome de Bartter [in French].** *Ann Endocrinol (Paris)* 1977, **38**:385–386.
4. Requeira O, Rao J, Baliga R: **Response to growth hormone in a child with Bartter's syndrome.** *Pediatr Nephrol* 1991, **5**:671–672.
5. Ruvalcaba RH, Martinez FE: **Case report: familial growth hormone deficiency associated with Bartter's syndrome.** *Am J Med Sci* 1992, **303**:411–414.
6. Boer LA, Zoppi G: **Bartter's syndrome with impairment of growth hormone secretion.** *Lancet* 1992, **340**:860.
7. Akil I, Ozen S, Kandiloglu AR, Ersoy B: **A patient with Bartter syndrome accompanying severe growth hormone deficiency and focal segmental glomerulosclerosis.** *Clin Exp Nephrol* 2010, **14**:278–282.
8. Buyukcelik M, Keskin M, Kilic BD, Kor Y, Balat A: **Bartter syndrome and growth hormone deficiency: three cases.** *Pediatr Nephrol* 2012, **27**:2145–2148.
9. Fukuyama S, Hiramatsu M, Akagi M, Higa M, Ohta T: **Novel mutations of the chloride channel Kb gene in two Japanese patients clinically**

diagnosed as Bartter syndrome with hypocalciuria. *J Clin Endocrinol Metab* 2004, **89**:5847–5850.
10. Nariai A, Yokoya S, Kato K: **A case of Bartter's syndrome with growth hormone deficiency [abstract].** *Clin Pediatr Endocrinol* 1993, **2**:165.
11. Ko CW, Koo JH: **Recombinant human growth hormone and Gitelman's syndrome.** *Am J Kidney Dis* 1999, **33**:778–781.
12. Bettinelli A, Rusconi R, Ciarmatori S, Righini V, Zammarchi E, Donati MA, Isimbaldi C, Bevilacqua M: **Gitelman disease associated with growth hormone deficiency, disturbances in vasopressin secretion and empty sella: a new hereditary renal tubular-pituitary syndrome?** *Pediatr Res* 1999, **46**:232–238.
13. Slyper AH: **Growth, growth hormone testing and response to growth hormone treatment in Gitelman syndrome.** *J Pediatr Endocrinol Metab* 2007, **20**:257–259.
14. Itagaki Y, Tagawa T, Fujii F, Tanabe Y, Sumi K, Nose O, Seino Y: **Bartter's syndrome with impairment of growth hormone secretion [abstract].** *Clin Pediatr Endocrinol* 1995, **4**:213.
15. Nariai A, Yokoya S, Tajima T: **Final height in two growth hormone-deficient patients with Bartter's syndrome treated with growth hormone in combination with luteinizing hormone-releasing hormone analog [abstract].** *Clin Pediatr Endocrinol* 2003, **12**:166.
16. Yokoyama T, Ohyanagi K: **A child case of Bartter syndrome with chronic renal failure treated by recombinant human hormones [abstract].** *Clin Pediatr Endocrinol* 1992, **1**:57.
17. Flyvbjerg A, Dørup I, Everts ME, Orskov H: **Evidence that potassium deficiency induces growth retardation through reduced circulating levels of growth hormone and insulin-like growth factor I.** *Metabolism* 1991, **40**:769–775.
18. Bogdanović R, Draaken M, Toromanović A, Dordević M, Stajić N, Ludwig M: **A novel CLCN5 mutation in a boy with Bartter-like syndrome and partial growth hormone deficiency.** *Pediatr Nephrol* 2010, **25**:2363–2368.
19. Mulatero P, Monticone S, Rainey WE, Veglio F, Williams TA: **Role of KCNJ5 in familial and sporadic primary aldosteronism.** *Nat Rev Endocrinol* 2013, **9**:104–112.

doi:10.1186/1752-1947-7-283
Cite this article as: Adachi *et al.*: Classic Bartter syndrome complicated with profound growth hormone deficiency: a case report. *Journal of Medical Case Reports* 2013 **7**:283.

PLOS ONE

Molecular and Clinical Studies in 138 Japanese Patients with Silver-Russell Syndrome

Tomoko Fuke[1,2], Seiji Mizuno[3], Toshiro Nagai[4], Tomonobu Hasegawa[2], Reiko Horikawa[5], Yoko Miyoshi[6], Koji Muroya[7], Tatsuro Kondoh[8], Chikahiko Numakura[9], Seiji Sato[10], Kazuhiko Nakabayashi[11], Chiharu Tayama[11], Kenichiro Hata[11], Shinichiro Sano[1,12], Keiko Matsubara[1], Masayo Kagami[1], Kazuki Yamazawa[1], Tsutomu Ogata[1,12]*

1 Department of Molecular Endocrinology, National Research Institute for Child Health and Development, Tokyo, Japan, **2** Department of Pediatrics, Keio University School of Medicine, Tokyo, Japan, **3** Department of Pediatrics, Central Hospital, Aichi Human Service Center, Aichi, Japan, **4** Department of Pediatrics, Dokkyo Medical University Koshigaya Hospital, Saitama, Japan, **5** Division of Endocrinology and Metabolism, National Center for Child Health and Development, Tokyo, Japan, **6** Department of Pediatrics, Osaka University Graduate School of Medicine, Suita, Japan, **7** Department of Endocrinology and Metabolism, Kanagawa Children's Medical Center, Kanagawa, Japan, **8** Division of Developmental Disability, Misakaenosono Mutsumi Developmental, Medical, and Welfare Center, Isahaya, Japan, **9** Department of Pediatrics, Yamagata University School of Medicine, Yamagata, Japan, **10** Department of Pediatrics, Saitama Municipal Hospital, Saitama, Japan, **11** Department of Maternal-Fetal Biology, National Research Institute for Child Health and Development, Tokyo, Japan, **12** Department of Pediatrics, Hamamatsu University School of Medicine, Hamamatsu, Japan

Abstract

Background: Recent studies have revealed relative frequency and characteristic phenotype of two major causative factors for Silver-Russell syndrome (SRS), i.e. epimutation of the *H19*-differentially methylated region (DMR) and uniparental maternal disomy 7 (upd(7)mat), as well as multilocus methylation abnormalities and positive correlation between methylation index and body and placental sizes in *H19*-DMR epimutation. Furthermore, rare genomic alterations have been found in a few of patients with idiopathic SRS. Here, we performed molecular and clinical findings in 138 Japanese SRS patients, and examined these matters.

Methodology/Principal Findings: We identified *H19*-DMR epimutation in cases 1–43 (group 1), upd(7)mat in cases 44–52 (group 2), and neither *H19*-DMR epimutation nor upd(7)mat in cases 53–138 (group 3). Multilocus analysis revealed hyper- or hypomethylated DMRs in 2.4% of examined DMRs in group 1; in particular, an extremely hypomethylated *ARHI*-DMR was identified in case 13. Oligonucleotide array comparative genomic hybridization identified a ~3.86 Mb deletion at chromosome 17q24 in case 73. Epigenotype-phenotype analysis revealed that group 1 had more reduced birth length and weight, more preserved birth occipitofrontal circumference (OFC), more frequent body asymmetry and brachydactyly, and less frequent speech delay than group 2. The degree of placental hypoplasia was similar between the two groups. In group 1, the methylation index for the *H19*-DMR was positively correlated with birth length and weight, present height and weight, and placental weight, but with neither birth nor present OFC.

Conclusions/Significance: The results are grossly consistent with the previously reported data, although the frequency of epimutations is lower in the Japanese SRS patients than in the Western European SRS patients. Furthermore, the results provide useful information regarding placental hypoplasia in SRS, clinical phenotypes of the hypomethylated *ARHI*-DMR, and underlying causative factors for idiopathic SRS.

Citation: Fuke T, Mizuno S, Nagai T, Hasegawa T, Horikawa R, et al. (2013) Molecular and Clinical Studies in 138 Japanese Patients with Silver-Russell Syndrome. PLoS ONE 8(3): e60105. doi:10.1371/journal.pone.0060105

Editor: Monica Miozzo, Università degli Studi di Milano, Italy

Received September 7, 2012; **Accepted** February 21, 2013; **Published** March 22, 2013

Funding: This work was funded by Grants-in-Aid for Scientific Research (A) (22249010) and Research (B) (21028026) from the Japan Society for the Promotion of Science (http://www.jsps.go.jp/english/index.html), by Grant for Research on Rare and Intractable Diseases (H24-042) from the Ministry of Health, Labor and Welfare (http://www.mhlw.go.jp/english/), and by Grant for National Center for Child Health and Development (23A-1) (http://www.ncchd.go.jp/English/Englishtop.htm). The funders had no role in study design, data collection and analysis, decision to publish, or preparation of the manuscript.

Competing Interests: The authors have declared that no competing interests exist.

* E-mail: tomogata@hama-med.ac.jp

Introduction

Silver-Russell syndrome (SRS) is a rare congenital developmental disorder characterized by pre- and postnatal growth failure, relative macrocephaly, triangular face, hemihypotrophy, and fifth-finger clinodactyly [1]. Recent studies have shown that epimutation (hypomethylation) of the paternally derived differentially methylated region (DMR) in the upstream of *H19* (*H19*-DMR) on chromosome 11p15.5 and maternal uniparental disomy for chromosome 7 (upd(7)mat) account for ~45% and 5–10% of SRS patients, respectively [1,2]. In this regard, phenotypic assessment has suggested that birth length and weight are more reduced and characteristic body features are more frequent in patients with *H19*-DMR epimutation than in those with upd(7)mat, whereas developmental delay tends to be more

frequent in patients with upd(7)mat than in those with *H19*-DMR epimutation [3,4]. Furthermore, consistent with the notion that imprinted genes play an essential role in placental growth and development [5], placental hypoplasia has been found in both *H19*-DMR epimutation and upd(7)mat [4,6], although comparison of placental weight has not been performed between *H19*-DMR hypomethylation and upd(7)mat. In addition, multilocus hypo- or hypermethylation and positive correlation between methylation index (MI, the ratio of methylated clones) and body and placental sizes have been reported in patients with *H19*-DMR epimutation [4,7–9], and several types of rare genomic alterations have been identified in a few of SRS patients [1,10–12].

Here, we report on molecular and clinical findings in 138 Japanese SRS patients, and discuss on the results obtained in this study.

Patients and Methods

Ethics statement

This study was approved by the Institutional Review Board Committee at the National Center for Child Health and Development. The parents of the affected children and the adult patients who can express an intention by themselves have given written informed consent to participate in this study and to publish their molecular and clinical data.

Patients

This study consisted of 138 Japanese patients (66 males and 72 females) with SRS phenotype aged 0–30 years (median 4.1 years), including 64 previously reported patients (20 patients with variable degrees of *H19*-DMR epimutation, three patients with upd(7)mat, one patient with 46,XY/46,XY,upd(7)mat mosaicism in whom upd(7)mat cells accounted for 91–92% of leukocytes and salivary cells and for 11% of placental tissue, and 40 patients of unknown cause) [4,6,13]. The 138 patients had a normal karyotype in all the ≥50 lymphocytes examined, and satisfied the selection criteria proposed by Netchine et al. [14], i.e., birth length and/or birth weight ≤ −2 standard deviation score (SDS) for gestational age as a mandatory criteria plus at least three of the following five features: (i) postnatal short stature (≤ −2 SDS) at 2 year of age or at the nearest measure available, (ii) relative macrocephaly at birth, i.e., SDS for birth length or birth weight minus SDS for birth occipitofrontal circumference (OFC) ≤ −1.5, (iii) prominent forehead during early childhood, (iv) body asymmetry, and (v) feeding difficulties during early childhood. Birth and present length/height, weight, and OFC were assessed by the gestational/postnatal age- and sex-matched Japanese reference data from the Ministry of Health, Labor, and Welfare and the Ministry of Education, Science, Sports and Culture. Placental weight was assessed by the gestational age-matched Japanese reference data [15]. Clinical features were evaluated by clinicians at different hospitals who participated in this study, using the same clinical datasheet. The SRS patients were classified into three groups by the molecular studies, i.e., those with *H19*-DMR hypomethylation (epimutation) (group 1), those with upd(7)mat (group 2), and the remaining patients (group 3).

Primers and samples

Primers utilized in this study are shown in Table S1. Leukocyte genomic DNA samples were examined in this study.

Methylation analysis

We performed pyrosequencing analysis for the *H19*-DMR encompassing the 6th CTCF (CCCTC-binding factor) binding site that functions as the primary regulator for the monoallelic *IGF2* and *H19* expressions [16–18], using bisulfite treated leukocyte genomic DNA samples of all the 138 patients. The procedure was as described in the manufacturer's instructions (Qiagen, Valencia, CA, USA). In brief, a 279 bp region was PCR-amplified with a primer set (PyF and PyR) for both methylated and unmethylated clones, and a sequence primer (SP) was hybridized to a single-stranded PCR products. Subsequently, the MIs were obtained for four CpG dinucleotides (CG5–CG7 and CG9), using PyroMark Q24 (Qiagen) (the MI for CG8 was not obtained, because the "C" residue of CG8 constitutes a C/T SNP) (Figure 1A). The PyF/PyR and SP were designed by PyroMark Assay Design Software Ver2.0. While the PyF sequence contains a SNP (*rs11564736*) with a mean minor allele frequency of 5% in multiple populations, the minor allele frequency is 0% in the Japanese as well as in the Asian populations (http://browser.1000genomes.org/Homo_sapiens/Variation/Population?db=core;r=11:2020801–2021801;v=rs11564736;vdb=variation;vf=7864021). Thus, we utilized this PyF.

We also carried out combined bisulfite restriction analysis (COBRA) for the *H19*-DMR. The methods were as described previously [4]. In short, a 435 bp region was PCR-amplified with a primer set (CoF and CoR) that hybridize to both methylated and unmethylated clones, and MIs were obtained for two CpG dinucleotides (CG5 and CG16) after digestion of the PCR products with methylated allele-specific restriction enzymes (*Hpy*188I and *Afl*III) (Figure 1A).

Thus, we could examine CG5 by both pyrosequencing and COBRA. While we also attempted to analyze CG16 by both methods, it was impossible to design an SP for the analysis of CG16 (although we could design an SP between CG11 and CG12, clear methylation data were not obtained for CG16, probably because of the distance between the SP and CG16).

In addition, we performed COBRA for the KvDMR1 in all the 138 patients (Figure S1A) because of the possibility that epimutation of the KvDMR1 could lead to SRS phenotype via some mechanism(s) such as overexpression of a negative growth regulator *CDKN1C* [19], and for multiple DMRs on various chromosomes in patients in whom relatively large amount of DNA samples were available, as reported previously [4,20,21]. To define the reference ranges of MIs (minimum ~ maximum), 50 control subjects were similarly studied with permission.

To screen upd(7)mat, PCR amplification was performed for the *MEST*-DMR on chromosome 7q32.2 in all the 138 patients, using methylated and unmethylated allele-specific PCR primer sets, as reported previously [6] (Figure 2A). In addition, bisulfite sequencing and direct sequencing for the primer binding sites for the *ARHI*-DMR analysis were performed in a patient (case 13) with an extremely low MI for the *ARHI*-DMR.

Microsatellite analysis

Microsatellite analysis was performed for four loci within a ~4.5 Mb telomeric 11p region (*D11S2071*, *D11S922*, *D11S1318*, and *D11S988*) in patients with hypomethylated *H19*-DMR, to examine the possibility of upd(11p)mat involving the *H19*-DMR. Microsatellite analysis was also carried out for nine loci widely dispersed on chromosome 7 (Table S2) in patients with abnormal methylation patterns of the *MEST*-DMR, to examine the possibility of upd(7)mat and to infer the underlying causes for upd(7)mat, i.e., trisomy rescue, gamete complementation, monosomy rescue, and post-fertilization mitotic error [22]. The methods have been reported previously [4,6].

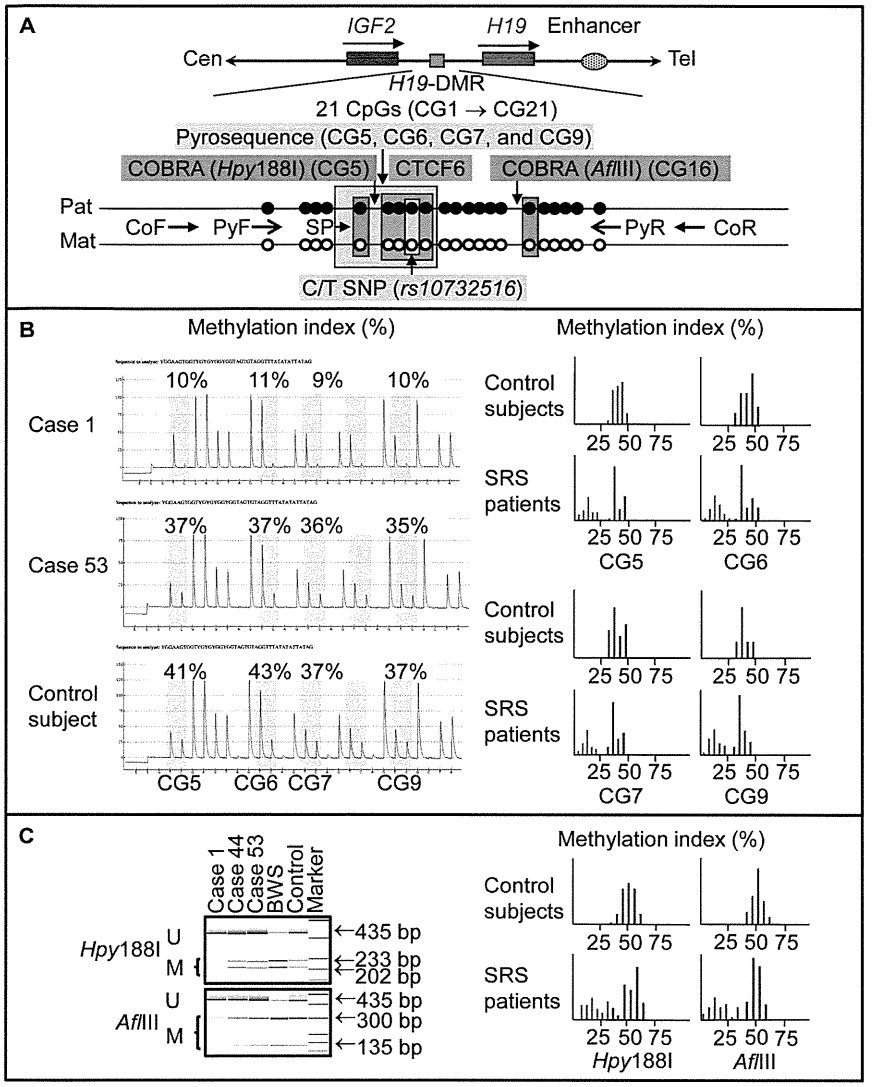

Figure 1. Methylation analysis of the *H19*-DMR, using bisulfite-treated genomic DNA. A. Schematic representation of a segment encompassing 21 CpG dinucleotides (CG1→CG21) within the *H19*-DMR. The cytosine residues at the CpG dinucleotides are usually methylated after paternal transmission (filled circles) and unmethylated after maternal transmission (open circles). The CTCF binding site 6 (CTCF6) is indicated with a blue rectangle; the cytosine residue at CG8 constitutes a C/T SNP (indicated with a gray rectangle). For pyrosequencing analysis, a 279 bp segment was PCR-amplified with PyF & PyR primers, and a sequence primer (SP) was hybridized to a single-stranded PCR products. Subsequently, the MIs were obtained for four CpG dinucleotides (CG5–CG7 and CG9) (indicated with a yellow rectangle). For COBRA, a 435 bp region was PCR-amplified with CoF & CoR primers, and the PCR product was digested with methylated allele-specific restriction enzymes to examine the methylation pattern of CG5 ands CG16 (the PCR products is digested with *Hpy*188I when the cytosine residue at CG5 is methylated and with *Afl*III when the cytosine residue at CG16 is methylated) (indicated with orange rectangles). *IGF2* is a paternally expressed gene, and *H19* is a maternally expressed gene. The stippled ellipse indicates the enhancer for *IGF2* and *H19*. B. Pyrosequencing data. Left part: Representative results indicating the MIs for CG5– CG7 and CG9. CG5– CG7 and CG9 are hypomethylated in case 1, and similarly methylated between case 53 and a control subject. Right part: Histograms showing the distribution of the MIs (the horizontal axis: the methylation index; and the vertical axis: the patient number). Forty-three SRS patients with low MIs are shown in red. C. COBRA data. Left part: Representative findings of PCR products loaded onto a DNA 1000 LabChip (Agilent, Santa Clara, CA, USA) after digestion with *Hpy*188I or *Afl*III. U: unmethylated clone specific bands; M: methylated clone specific bands; and BWS: Beckwith-Wiedemann syndrome patient with upd(11p15)pat. Right part: Histograms showing the distribution of the MIs.
doi:10.1371/journal.pone.0060105.g001

Oligoarray comparative genomic hybridization (CGH)

We performed oligoarray CGH in the 138 SRS patients, using a genomewide 4×180K Agilent platform catalog array and a custom-build high density oligoarray for the 11p15.5, 7p12.2, 12q14, and 17q24 regions where rare copy number variants have been identified in several SRS patients [1,10–12] as well as for the 7q32–qter region involved in the segmental upd(7)mat in four SRS patients [23–25]. The custom-build high density oligoarray contained 3,214 probes for 7p12.2, 434 probes for 7q32, 23,162 probes for 12q14, and 39,518 probes for 17q24, together with ~10,000 reference probes for other chromosomal region (Agilent Technologies, Palo Alto, CA, USA). The procedure was as described in the manufacturer's instructions.

Statistical analysis

After examining normality by χ^2 test, the variables following the normal distribution were expressed as the mean±SD, and those not following the normal distribution were expressed with the

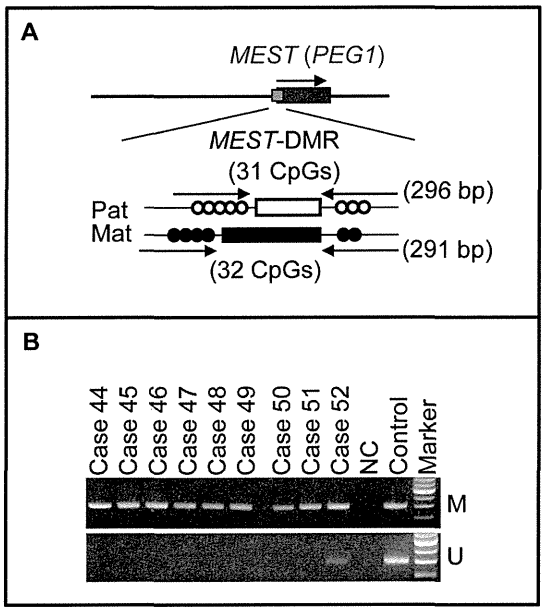

Figure 2. Methylated and unmethylated allele-specific PCR analysis for the *MEST*-DMR. A. Schematic representation of the *MEST*-DMR. The cytosine residues at the CpG dinucleotides are usually unmethylated after paternal transmission (open circles) and methylated after maternal transmission (filled circles). The PCR primers have been designed to hybridize either methylated or unmethylated clones. B. The results of methylation analysis with methylated and unmethylated allele-specific primers.
doi:10.1371/journal.pone.0060105.g002

median and range. Statistical significance of the mean was analyzed by Student's *t*-test or Welch's *t*-test after comparing the variances by *F* test, that of the median by Mann-Whitney's *U*-test, that of the frequency by Fisher's exact probability test, and that of the correlation by Pearson's correlation coefficient after confirming the normality of the variables. $P<0.05$ was considered significant.

Results

Identification of *H19*-DMR hypomethylation

Representative findings are shown in Figure 1B and 1C, and the MIs are summarized in Table 1. Overall, the MIs obtained by the pyrosequencing analysis tended to be lower and distributed more narrowly than those obtained by the COBRA. Despite such difference, the MIs obtained by the pyrosequencing analysis for CG5–CG7 and CG9 and by the COBRA for CG5 and CG16 were invariably below the normal range in the same 43 patients (cases 1–43) (group 1). By contrast, the MIs were almost invariably within the normal range in the remaining 95 patients, while the MIs obtained by the pyrosequencing analysis slightly (1–2%) exceeded the normal range in the same three patients (cases 136–138).

In the 43 cases of group 1, microsatellite analysis for four loci at the telomeric 11p region excluded maternal upd in 14 cases in whom parental DNA samples were available; in the remaining 29 cases, microsatellite analysis identified two alleles for at least one locus, excluding maternal uniparental isodisomy for this region. Furthermore, oligoarray CGH for the chromosome 11p15.5 region showed no copy number alteration such as duplication of maternally derived *H19*-DMR and deletion of paternally derived *H19*-DMR. For the KvDMR1, the MIs of the 138 patients remained within the reference range (Fig. S1B and C).

Table 1. The methylation indices (%) for the *H19*-DMR.

	Cases 1–43	Cases 44–138	Control subjects
Pyrosequencing analysis			
CG5	4–24	35–50	33–48
CG6	5–26	36–53	34–51
CG7	4–24	35–49	30–47
CG9	5–23	34–48	30–46
COBRA			
CG5 (*Hpy*188I)	3.3–35.1	37.8–60.8	36.2–58.5
CG16 (*Afl*III)	4.1–35.0	43.0–59.4	38.7–60.0

The position of examined CpG dinucleotides (CG5–7, CG9, and CG16) is shown in Figure 1A.
COBRA: combined bisulfite restriction analysis.
doi:10.1371/journal.pone.0060105.t001

Identification of upd(7)mat

Methylation analysis for the *MEST*-DMR revealed that unmethylated bands were absent from eight patients and remained faint in a single patient (cases 44–52) (group 2) (Figure 2B). Subsequent microsatellite analysis confirmed upd(7)mat in the eight patients and mosaic upd(7)mat in the remaining one patient, and indicated trisomy rescue or gamete complementation type upd(7)mat in cases 44–48, monosomy rescue or post-fertilization mitotic error type upd(7)mat in cases 49–51, and post-fertilization mitotic error type mosaic upd(7)mat in case 52 (Table S2).

Multiple DMR analysis

We examined 17 autosomal DMRs other than the *H19*-DMR in 14 patients in group 1, four patients in group 2, and 20 patients in group 3, and the *XIST*-DMR in eight female patients in group 1, one female patient in group 2, and five female patients in group 3 (Table S3). The MIs outside the reference ranges were identified in five of 14 examined cases (35.7%) and six of a total of 246 examined DMRs (2.4%) in group 1. In particular, a single case with the mean MI value of 23 obtained by the pyrosequencing analysis for CG5–CG7 and CG9 had an extremely low MI for the *ARHI*-DMR (case 13 of group 1). This extreme hypomethylation was confirmed by bisulfite sequencing, and direct sequencing showed normal sequences of the primer-binding sites, thereby excluding the possibility that such an extremely low MI could be due to insufficient primer hybridization because of the presence of a nucleotide variation within the primer-binding sites (Figure 3). Furthermore, no copy number variation involving the *ARHI*-DMR was identified by CGH analysis using a genomewide catalog array. Consistent with upd(7)mat, three DMRs on chromosome 7 were extremely hypermethylated in four examined cases of group 2. Only a single DMR was mildly hypermethylated in a total of 345 examined DMRs in group 3. The abnormal MIs, except for those for the *H19*-DMR in group 1 and for the three DMRs on chromosome 7 in group 2, were confirmed by three times experiments.

Oligonucleotide array CGH

A ~3.86 Mb deletion at chromosome 17q24 was identified in a single patient (case 73 of group 3) (Figure 4).

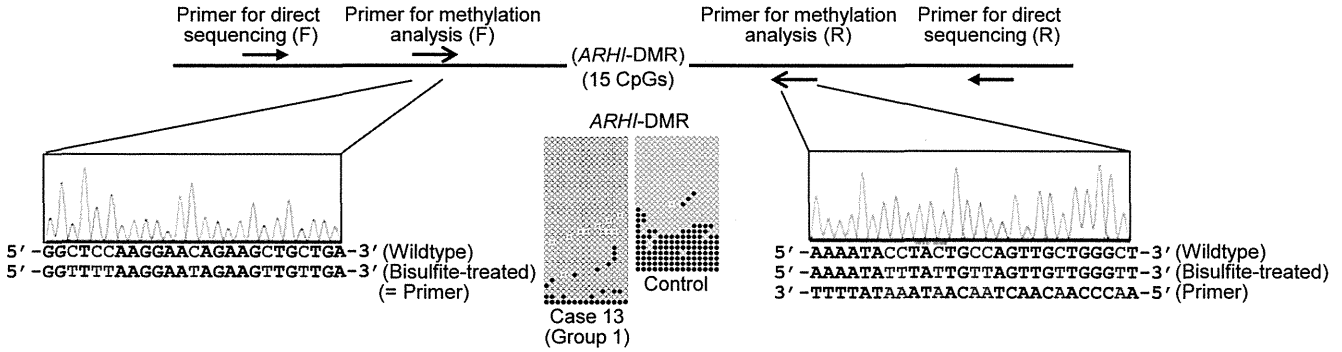

Figure 3. Analysis of the *ARHI*-DMR in case 13. For bisulfite sequencing, each line indicates a single clone, and each circle denotes a CpG dinucleotide; the cytosine residues at the CpG dinucleotides are usually unmethylated after paternal transmission (open circles) and methylated after maternal transmission (filled circles). Electrochromatograms delineate the sequences of the primer binding sites utilized for the methylation analysis.
doi:10.1371/journal.pone.0060105.g003

Epigenotype-phenotype analysis

Clinical findings of SRS patients in groups 1–3 are summarized in Table 2. All the patients met the mandatory criteria, and most patients in each group had severely reduced birth length and weight (both≦–2 SDS). For the five clinical features utilized as scoring system criteria, while 23.2% of patients in group 1 and 22.2% of patients in group 2 exhibited all the five features, there was no patient in group 3 who was positive for all the five features. By contrast, while 39.5% of patients in group 1 and 33.3% of patients in group 2 manifested just three of the five features, 77.6% of patients in group 3 were positive for just three features. In particular, the frequencies of relative macrocephaly at birth and body asymmetry were low in group 3, while those of the remaining three scoring system criteria including prominent forehead during early childhood were similar among groups 1–3.

Phenotypic comparison between groups 1 and 2 revealed that birth length and weight were more reduced and birth OFC was more preserved in group 1 than in group 2, despite comparable gestational age. In the postnatal life, present height and weight became similar between the two groups, whereas present OFC became significantly smaller in group 1 than in group 2. Body asymmetry and brachydactyly were more frequent and speech delay was less frequent in group 1 than in group 2. Placental weight was similar between the two groups, and became more similar after excluding case 52 with mosaic upd(7)mat (see legends for Table 2). Parental age at childbirth was also similar between the two groups. In group 2, placental weight was grossly similar among examined cases, as was parental age at childbirth (see legends for Table 2).

Case 13 with an extremely low MI for the *ARHI*-DMR and case 73 with a cryptic deletion at chromosome 17q24 had no specific phenotype other than SRS-like phenotype (Table S4). However, of the five clinical features utilized as scoring system criteria, all the five features were exhibited by case 13 and just three features were

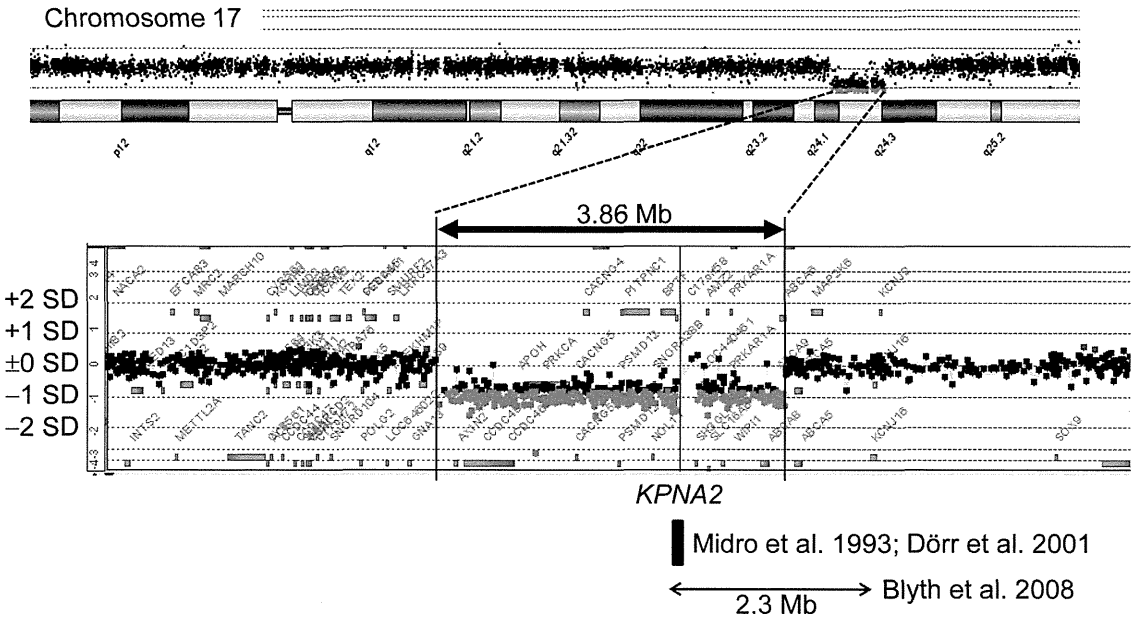

Figure 4. Oligonucleotide array CGH in case 73, showing a ~3.86 Mb deletion at chromosome 17q24. The black, the red, and the green dots denote signals indicative of the normal, the increased(>+0.5), and the decreased (< –1.0) copy numbers, respectively. The horizontal bar with arrowheads indicates a ~2.3 Mb deletion identified in a patient with Carney complex and SRS-like phenotype [44], and the black square represent a ~65 kb segment harboring the breakpoint of a *de novo* translocation 46,XY,t(1;17)(q24;q23–q24) identified in a patient with SRS phenotype [45,46].
doi:10.1371/journal.pone.0060105.g004

Table 2. Phenotypic comparison in three groups of patients with Silver-Russell syndrome.

	H19-DMR hypomethylation	Upd(7)mat	Unknown	*P*-value		
	(Group 1)	(Group 2)	(Group 3)	G1 vs. G2	G1 vs. G3	G2 vs. G3
Patient number	43 (31.2%)	9 (6.5%)	85 (62.0%)			
Mandatory criteria	43/43 (100%)	9/9 (100%)	85/85 (100%)	1.000	1.000	1.000
Scoring system criteria (5/5)	10/43 (23.2%)	2/9 (22.2%)	0/85 (0.00%)	0.965	**1.52×10^{-4}**	**2.58×10^{-2}**
Scoring system criteria (4/5)	16/43 (37.2%)	4/9 (44.4%)	19/85 (22.4%)	0.792	**1.45×10^{-2}**	0.145
Scoring system criteria (3/5)	17/43 (39.5%)	3/9 (33.3%)	66/85 (77.6%)	0.821	**7.17×10^{-4}**	0.161
Gestational age (weeks:days)	38:0 (34:3~40:0) (n = 36)	38:0 (34:4~40:0) (n = 9)	37:6 (27:1~41:4) (n = 65)	0.877	0.120	0.450
BL (SDS)	−4.13±2.01 (n = 31)	−3.18±1.16 (n = 9)	−2.93±1.43 (n = 60)	**2.67×10^{-2}**	**6.69×10^{-5}**	0.619
BW (SDS)	−3.50±0.85 (n = 42)	−2.90±0.64 (n = 9)	−2.71±1.14 (n = 64)	**3.28×10^{-2}**	**5.87×10^{-4}**	0.640
BL≤−2 SDS and/or BW≤−2 SDS*	43/43 (100%)	9/9 (100%)	85/85 (100%)	1.000	1.000	1.000
BL≤−2 SDS and BW≤−2 SDS	39/43 (90.7%)	7/9 (77.8%)	76/85 (89.4%)	0.474	0.821	0.304
BOFC (SDS)	−0.54±1.22 (n = 29)	−1.44±0.47 (n = 9)	−1.92±1.09 (n = 48)	**3.74×10^{-2}**	**1.52×10^{-6}**	0.202
BL (SDS) − BOFC (SDS)	−3.70±2.02 (n = 27)	−1.73±1.20 (n = 9)	−0.943±1.48 (n = 43)	**1.02×10^{-2}**	**3.40×10^{-9}**	0.111
BW (SDS) − BOFC (SDS)	−3.21±1.20 (n = 27)	−1.53±0.57 (n = 9)	−1.04±1.55 (n = 48)	0.326	**7.38×10^{-9}**	0.331
Relative macrocephaly at birth† BL or BW (SDS) − BOFC (SDS)≤−1.5	29/29 (100%)	7/9 (77.8%)	16/45 (35.6%)	0.341	**3.67×10^{-8}**	**2.05×10^{-2}**
Present age (years:months)	4.1 (0:6~30:6) (n = 31)	4.8 (2:4~25:2) (n = 9)	4.3 (0:1~18:6) (n = 60)	0.437	0.813	0.335
PH (SDS)	−3.58±1.65 (n = 35)	−3.77±1.13 (n = 9)	−3.17±1.50 (n = 61)	0.757	0.218	0.253
PH≤−2 SDS (≥2 years)†	29/35 (82.5%)	8/9 (88.9%)	52/61 (85.2%)	0.760	0.758	0.772
PW (SDS)	−3.15±1.16 (n = 32)	−2.77±0.76 (n = 9)	−2.77±1.34 (n = 59)	0.362	0.144	0.968
POFC (SDS)	−1.16±1.18 (n = 21)	−0.01±0.91 (n = 9)	−1.81±1.57 (n = 35)	**2.01×10^{-3}**	0.107	**3.08×10^{-3}**
PH (SDS) − POFC (SDS)	−2.47±1.63 (n = 16)	−3.62±1.38 (n = 8)	−1.55±1.82 (n = 35)	0.103	**4.39×10^{-2}**	**1.64×10^{-2}**
PW (SDS) − POFC (SDS)	−2.84±1.31 (n = 21)	−2.69±1.36 (n = 9)	−1.08±1.71 (n = 35)	0.782	**2.54×10^{-2}**	**1.90×10^{-4}**
Relative macrocephaly at present PH or PW (SDS) − POFC (SDS)≤−1.5	20/21 (95.2%)	8/8 (100%)	29/43 (67.4%)	0.223	**4.77×10^{-3}**	0.156
Triangular face during early childhood	42/43 (97.7%)	8/9 (88.9%)	65/65 (100%)	0.442	0.0773	**5.98×10^{-3}**
Prominent forehead during early childhood†	31/37 (83.8%)	7/9 (100%)	41/53 (77.4%)	0.200	0.456	0.978
Ear anomalies	14/35 (40.0%)	3/9 (33.3%)	15/55 (27.3%)	0.717	0.290	0.823
Irregular teeth	12/26 (46.2%)	4/9 (44.4%)	12/45 (26.7%)	0.930	0.0968	0.291
Body asymmetry†	30/37 (81.1%)	3/9 (33.3%)	19/59 (32.2%)	**4.77×10^{-3}**	**3.51×10^{-6}**	0.947
Clinodactyly	29/37 (78.4%)	5/9 (55.6%)	50/58 (86.2%)	0.167	0.323	**2.68×10^{-2}**
Brachydactyly	30/38 (78.9%)	2/9 (22.2%)	34/56 (60.7%)	1.16×10^{-3}	0.0642	**3.24×10^{-2}**
Syndactyly	3/36 (8.3%)	0/9 (0.00%)	3/52 (5.77%)	0.375	0.641	0.464
Simian crease	4/26 (15.4%)	2/7 (28.6%)	6/49 (12.2%)	0.429	0.705	0.252
Muscular hypotonia	17/32 (53.1%)	5/9 (55.6%)	12/50 (24.0%)	0.898	**7.49×10^{-3}**	0.0564
Developmental delay	18/37 (48.6%)	6/9 (66.7%)	25/54 (46.3%)	0.337	0.826	0.262
Speech delay	8/31 (25.8%)	6/9 (66.7%)	18/43 (41.9%)	**2.55×10^{-2}**	0.156	0.179
Feeding difficulty†	16/34 (47.1%)	6/9 (66.7%)	25/51 (49.0%)	0.301	0.860	0.333
Placental weight (SDS)	−2.10±0.74 (n = 14)	−1.72 ± 0.74 (n = 6)[a]	−1.02±0.86 (n = 18)	0.312	**4.12×10^{-3}**	**8.24×10^{-3}**
Paternal age at childbirth (years:months)	32:0 (19:0~52:0) (n = 24)	35:0 (27:0~48:0) (n = 9)	32:0 (25:0~46:0) (n = 45)	0.223	1.00	0.105
Maternal age at childbirth (years:months)	32:0 (19:0~43:0) (n = 25)	33:0 (25:0~42:0) (n = 9)[b]	30:0 (22:0~43:0) (n = 46)	0.275	0.765	0.117

BL: birth length; BW: birth weight; BOFC: birth occipitofrontal circumference; PH: present height; PW: present weight; POFC: present occipitofrontal circumference, and SDS: standard deviation score.

For body features, the denominators indicate the number of patients examined for the presence or absence of each feature, and the numerators represent the number of patients assessed to be positive for that feature.

*Mandatory criteria and †five clinical features utilized as selection criteria for Silver-Russell syndrome proposed by Netchine et al. [14].

Significant *P*-values(<0.05) are boldfaced.

[a]Placental weight SDS is −1.68, −2.55, −2.24, −1.12, −2.14 and −0.60 in case 46, 47, 49, 50, 51 and 52, respectively; the placental weight SDS is −1.95±0.57 in five cases except for case 52 with mosaic upd(7)mat.

[b]Maternal childbearing age is 32, 32, 33, 42, 32, 34, 33, 25 and 36 years in case 44–52, respectively.

doi:10.1371/journal.pone.0060105.t002

manifested by case 73. In addition, cases 136–138 with slightly elevated MIs for CG5–CG7 and CG9, and cases with multilocus methylation abnormalities, had no particular phenotype other than SRS-compatible clinical features.

Correlation analysis

In group 1, the mean value of the MIs for CG5–CG7 and CG9 obtained by pyrosequencing analysis was positively correlated with the birth length and weight, the present height and weight, and the placental weight, but with neither the birth nor the present OFC (Table 3). Such correlations with the growth parameters were grossly similar but somewhat different for the MIs obtained by COBRA (Table S5). Furthermore, the placental weight was positively correlated with the birth weight and length, but not with the birth OFC. Such positive correlations were not found in groups 2 and 3.

Discussion

The present study identified hypomethylation of the *H19*-DMR and upd(7)mat in 31.2% and 6.5% of 138 Japanese SRS patients, respectively. In this regard, the normal KvDMR1 methylation patterns indicate that the aberrant methylation in 43 cases of group 1 is confined to the *H19*-DMR. Furthermore, oligoarray CGH excludes copy number variants involving the *H19*-DMR, and microsatellite analysis argues against segmental maternal isodisomy that could be produced by post-fertilization mitotic error [26]. These findings imply that the *H19*-DMR hypomethylation is due to epimutation (hypomethylation of the normally methylated *H19*-DMR of paternal origin).

The frequency of epimutations detected in this study is lower than that reported in Western European SRS patients [1,2,14], although the frequency of upd(7)mat is grossly similar between the two populations [2,11,14,27,28]. In this context, it is noteworthy that, of the five scoring system criteria, the frequencies of relative macrocephaly at birth and body asymmetry were low in group 3, while those of the remaining three scoring system criteria were similar among groups 1–3. Since relative macrocephaly and body asymmetry are characteristic of *H19*-DMR epimutation, the lack of these two features in a substantial fraction of cases in group 3 would primarily explain the low frequency of *H19*-DMR epimutations in this study. In group 3, furthermore, the low prevalence of relative macrocephaly at birth appears to be discordant with the high prevalence of prominent forehead during early childhood. Since relative macrocephaly was evaluated by an objective method (SDS for birth length or birth weight minus SDS for birth OFC≤−1.5) and prominent forehead was assessed by a subjective impression of different clinicians, it is recommended to utilize relative macrocephaly as a more important and reliable feature in the scoring system than prominent forehead. In addition, the difference in the ethnic group might also be relevant to the low frequency of *H19*-DMR epimutations in this study.

Table 3. Correlation analyses in patients with *H19*-DMR hypomethylations.

Parameter 1	Parameter 2	*r*	*P*-value
Methylation index (%)* vs.	Birth length (SDS)	0.647	**6.70×10^{-3}**
	Birth weight (SDS)	0.590	**7.80×10^{-3}**
	Birth OFC (SDS)	0.190	0.498
	Present height (SDS)	0.612	**5.33×10^{-3}**
	Present weight (SDS)	0.605	**7.81×10^{-3}**
	Present OFC (SDS)	−0.166	0.647
	Placental weight (SDS)	0.809	**8.30×10^{-3}**
Placental weight (SDS) vs.	Birth weight (SDS)	0.717	**8.64×10^{-3}**
	Birth length (SDS)	0.636	**2.63×10^{-2}**
	Birth OFC (SDS)	0.400	0.198

SDS: standard deviation score; and OFC: occipitofrontal circumference.
*The mean value of MIs for CG5, CG6, CG7, and CG9 obtained by pyrosequencing analysis.
Significant *P*-values(<0.05) are boldfaced.
doi:10.1371/journal.pone.0060105.t003

Epigenotype-phenotype correlations in this study are grossly similar to those previously reported in Western European SRS patients [1–3]. Cases 1–43 in group 1 with *H19*-DMR epimutation had more reduced birth weight and length, more preserved birth OFC and more reduced present OFC, more frequent body features, and less frequent speech delay than case 44–52 in group 2 with upd(7)mat, although the difference in the prevalence of somatic features appears to be less remarkable in this study than in the previous studies [3,4]. This provides further support for the presence of relatively characteristic clinical features in *H19*-DMR epimutation and upd(7)mat [1–3]. In this context, previous studies have indicated biallelic *IGF2* expression in the human fetal choroid plexus, cerebellum, and brain, and monoallelic *IGF2* expression in the adult brain, while the precise brain tissue(s) with such a unique expression pattern remains to be clarified [29,30,31]. This may explain why the birth OFC is well preserved and the present OFC is reduced in group 1. However, since the difference in present OFC between groups 1 and 2 is not necessarily significant in the previous studies [32], the postnatal OFC growth awaits further investigations.

Placental weight was similarly reduced in groups 1 and 2. Thus, placental weight is unlikely to represent an indicator for the discrimination between the two groups, although the present data provide further support for imprinted genes being involved in placental growth, with growth-promoting effects of *PEGs* and growth-suppressing effects of *MEGs* [5,6]. It should be pointed out, however, that the placental hypoplasia could be due to some other genetic or environmental factor(s). In particular, while placental weight was apparently similar among cases of group 2, possible confined placental mosaicism [33,34] with trisomy for chromosome 7 may have exerted some effects on placental growth in cases with trisomy rescue type upd(7)mat.

Correlation analysis would imply that the *IGF2* expression level, as reflected by the MI of the *H19*-DMR, plays a critical role in the determination of pre- and postnatal body (stature and weight) and placental growth in patients with *H19*-DMR epimutation. Since the placental weight was positively correlated with the birth length and weight, the reduced *IGF2* expression level appears to have a similar effect on the body and the placental growth. Furthermore, the lack of correlations between the MI and birth and present OFC and between placental weight and birth OFC would be compatible with the above mentioned *IGF2* expression pattern in the central nervous system [29]. Although the MI would also reflect the *H19* expression level, this would not have a major growth effect. It has been implicated that *H19* functions as a tumor suppressor [35,36].

Multilocus analysis revealed co-existing hyper- and hypomethylated DMRs predominantly in cases of group 1, with frequencies of 35.7% of examined patients and 2.4% of examined DMRs. The results are grossly consistent with the previous data indicating that co-existing abnormal methylation patterns of DMRs are almost exclusively identified in patients with *H19*-DMR epimutation with frequencies of 9.5~30.0% of analyzed patients and 1.8~5.2% of a